Matter and Radiation at Extremes | REGULAR ARTICLE | scitation.org/journal/mre

Photon polarization effects in polarized electron–positron pair production in a strong laser field

Cite as: Matter Radiat. Extremes 7, 014401 (2022); doi: 10.1063/5.0063633
Submitted: 16 July 2021 • Accepted: 8 October 2021 •
Published Online: 23 November 2021

Ya-Nan Dai,[1] Bai-Fei Shen,[1,2] Jian-Xing Li,[3] Rashid Shaisultanov,[4,5] Karen Z. Hatsagortsyan,[4] Christoph H. Keitel,[4] and Yue-Yue Chen[1,a)]

AFFILIATIONS

[1]Department of Physics, Shanghai Normal University, Shanghai 200234, China
[2]State Key Laboratory of High Field Laser Physics and CAS Center for Excellence in Ultra-intense Laser Science, Shanghai Institute of Optics and Fine Mechanics (SIOM), Chinese Academy of Sciences (CAS), Shanghai 201800, China
[3]School of Physics, Xi'an Jiaotong University, Xi'an 710049, China
[4]Max-Planck-Institut fur Kernphysik, Saupfercheckweg 1, 69117 Heidelberg, Germany
[5]Helmholtz-Zentrum Dresden-Rossendorf, Bautzner Landstraße 400, 01328 Dresden, Germany

[a)]**Author to whom correspondence should be addressed:** yueyuechen@shnu.edu.cn

ABSTRACT

Deep understanding of the impact of photon polarization on pair production is essential for the efficient generation of laser-driven polarized positron beams and demands a complete description of polarization effects in strong-field QED processes. Employing fully polarization-resolved Monte Carlo simulations, we investigate correlated photon and electron (positron) polarization effects in the multiphoton Breit–Wheeler pair production process during the interaction of an ultrarelativistic electron beam with a counterpropagating elliptically polarized laser pulse. We show that the polarization of e^-e^+ pairs is degraded by 35% when the polarization of the intermediate photon is resolved, accompanied by an ~13% decrease in the pair yield. Moreover, in this case, the polarization direction of energetic positrons at small deflection angles can even be reversed when high-energy photons with polarization parallel to the laser electric field are involved.

I. INTRODUCTION

Polarized positron beams are a powerful tool for exploration of the fine structure of matter, particularly for probing nuclear constituents[1] and for testing the validity of the Standard Model[2] of particle physics via weak and electromagnetic interactions. The natural decay of some radioisotopes generates polarized positrons with polarization up to 40%,[3] but the flux is too low for further acceleration and applications. Positrons can also be polarized in a storage ring by spin-flips at photon emissions (the Sokolov–Ternov effect),[4–8] but this is a slow process lasting at least several minutes and can only be realized in large-scale storage ring facilities. At particle accelerators, polarized e^-e^+ pairs are commonly produced by scattering of circularly polarized gamma photons in a high-Z material via the Bethe–Heitler process,[9–11] but the luminosity of the positrons is limited because of constraints on the target thickness,[12] and the required intense flux of sufficiently energetic photons with a high degree of circular polarization is challenging to produce.[13]

Recently, the rapid development of petawatt (PW) laser technology[14–19] and laser wakefield acceleration[20,21] have stimulated a considerable amount of interest in the development of a polarized positron source via the nonlinear Breit–Wheeler (NBW) process.[22–29] Positrons created in a strong laser field can be polarized owing to the energetically preferred orientation of the positron spin along the local magnetic field. However, the challenge is that in a symmetric laser field (e.g., in a monochromatic laser field), the polarization of positrons created in different laser half-cycles oscillates following the laser magnetic field and averages out to zero for the total beam. Thus, to achieve net polarization of the created positrons, it is necessary to use an asymmetric laser field. For instance, a two-color laser field has recently been proposed to exploit the ultrafast generation of highly polarized

electron[30,31] and positron beams.[24] Another efficient method for laser-driven generation of polarized electrons (or positrons) has been also demonstrated,[23,32] in which the spin-dependent radiation reaction in an elliptically polarized laser pulse is employed to split the electron (or positron) beam into two oppositely transversely polarized parts. Laser-driven positron generation schemes provide a promising avenue for the development of high-current, highly polarized positron sources.

Usually the gamma photon that creates a pair in the NBW process is generated by Compton scattering of the incoming electron beam off a counterpropagating laser field. In most studies, the gamma photon has been assumed to be unpolarized, and the NBW probability has been averaged over the photon polarization.[23,24,30,31] In reality, the intermediate gamma photon is partially polarized, which has consequences for further pair production processes.[25,33,34] In particular, the decrease in pair density with the inclusion of photon polarization has been shown in analytical QED calculations[33] averaged by the lepton spins, which is confirmed by more accurate spin-resolved Monte Carlo simulations.[34] Moreover, highly polarized gamma photons can be obtained with polarized seed electrons,[13] which in further NBW process may create highly polarized positrons, as has been shown in Monte Carlo simulations[25] with the use of a simplified pair production probability summed up over final spin states of either electron or positron. A recent study has shown that arbitrarily polarized lepton beams can be obtained by controlling the polarization of gamma-ray beams and laser configurations in the NBW process.[35] Therefore, including photon polarization in the description of the NBW process is mandatory for reliable prediction of the parameters of a laser-driven polarized positron source. The study of fully polarization resolved NBW is also of pure fundamental interest, providing insight into correlations of electron, positron, and photonspolarization in strong-field pair production processes.

An accurate analytical description of strong-field QED processes is possibly only in the case of a plane wave laser field.[22,36–40] For QED processes in more realistic scenarios, including focused laser fields and laser–plasma interaction, a Monte Carlo method has been developed[41–43] that is based on the local constant field approximation (LCFA)[44–50] applicable to intense laser–plasma[41–43,51]/ultrarelativistic electron interactions.[13,24,25,34] Recently, the QED Monte Carlo method has been generalized to include the spin of involved leptons[24,32] and the polarization of emitted or absorbed photons.[13,25,34,52] A numerical approach suitable for treating polarization effects beyond the LCFA and plane wave approximations at intermediate laser intensities has been developed[53,54] for strong-field pair production processes within the semiclassical Baier–Katkov formalism.

In this paper, we investigate the interaction of an ultrarelativistic electron beam colliding head-on with an ultraintense laser pulse and focus on the effects of photon polarization in NBW pair production processes. To provide an accurate analysis of the produced pair polarization, we employ fully polarization-resolved NBW probabilities, i.e., resolved in incoming photon polarization as well as in the created electron and positron polarizations. The probabilities are derived using the Baier–Katkov QED operator method[44,55] within the LCFA and have been included in a recently developed laser–electron beam simulation code.[25] We consider a scheme where the initial electrons are transversely polarized and the laser field is elliptically polarized. With the fully polarization-resolved Monte Carlo method, we find that the polarization of the produced positrons is highly dependent on the polarization of the parent photons. In particular, we find that the polarization of positrons is reduced by 35%, since the emitted photons are partially polarized along the electric field direction, and that the angular distribution of positron polarization exhibits an abnormal twist near the small-angle region, which originates from pair production of highly polarized photons at the high-energy end of the spectrum.

II. SIMULATION METHOD

In this section, we analyze the correlation of photon and positron/electron polarization based on fully polarization-resolved probabilities and briefly elaborate on the Monte Carlo method used for our simulation.

A. Photon-polarization-resolved radiation probability

Here, we provide probabilities of a polarized photon emission with a polarized electron. Let us assume that the polarization of the emitted photon is $\vec{e} = a_1\vec{e}_1 + a_2\vec{e}_2$, where

$$\vec{e}_1 = \vec{s} - \vec{n}\left(\vec{n}\cdot\vec{s}\right), \qquad \vec{e}_2 = \vec{n}\times\vec{e}_1. \tag{1}$$

$\vec{n} = \vec{k}/|\vec{k}|$ and $\vec{s} = \vec{w}/|\vec{w}|$ are the unit vectors along the photon emission and acceleration directions, respectively. The photon-polarization-resolved emission probability is[13]

$$\begin{aligned} dW_r &= \frac{1}{2}\left(dW_{11}+dW_{22}\right) + \frac{1}{2}\xi_1\left(dW_{11}-dW_{22}\right) \\ &\quad - i\frac{1}{2}\xi_2\left(dW_{21}-dW_{12}\right) + \frac{1}{2}\xi_3\left(dW_{11}-dW_{22}\right) \\ &= \frac{1}{2}\left(F_0 + \xi_1F_1 + \xi_2F_2 + \xi_3F_3\right), \end{aligned} \tag{2}$$

where $\xi_i\,(i=1,2,3)$ are the Stokes parameters with respect to the axes $(\vec{e}_1, \vec{e}_2, \vec{n})$, and

$$\begin{aligned} F_0 = \frac{\alpha}{2\sqrt{3}\pi\gamma^2}\,d\omega\,\Bigg\{ & \left[\frac{\varepsilon^2+\varepsilon'^2}{\varepsilon\varepsilon'}\mathrm{K}_{2/3}\left(z_q\right) - \int_{z_q}^{\infty}dx\,\mathrm{K}_{1/3}\left(x\right)\right] \\ & + \left[2\mathrm{K}_{2/3}\left(z_q\right) - \int_{z_q}^{\infty}dx\,\mathrm{K}_{1/3}\left(x\right)\right]\left(\vec{\zeta}_i\cdot\vec{\zeta}_f\right) \\ & - \mathrm{K}_{1/3}\left(z_q\right)\left[\frac{\omega}{\varepsilon}\left(\vec{\zeta}_i\cdot\vec{b}\right) + \frac{\omega}{\varepsilon'}\left(\vec{\zeta}_f\cdot\vec{b}\right)\right] \\ & + \frac{\omega^2}{\varepsilon'\varepsilon}\left[\mathrm{K}_{2/3}\left(z_q\right) - \int_{z_q}^{\infty}dx\,\mathrm{K}_{1/3}\left(x\right)\right]\left(\vec{\zeta}_i\cdot\vec{\nu}\right)\left(\vec{\zeta}_f\cdot\vec{\nu}\right)\Bigg\}, \end{aligned} \tag{3}$$

$$\begin{aligned} F_1 = \frac{\alpha}{2\sqrt{3}\pi\gamma^2}\,d\omega\,\Bigg\{ & \frac{\varepsilon^2-\varepsilon'^2}{2\varepsilon'\varepsilon}\mathrm{K}_{2/3}\left(z_q\right)\left[\vec{\nu}\cdot\left(\vec{\zeta}_f\times\vec{\zeta}_i\right)\right] \\ & + \left[\frac{\omega}{\varepsilon'}\left(\vec{\zeta}_i\cdot\vec{s}\right) + \frac{\omega}{\varepsilon}\left(\vec{\zeta}_f\cdot\vec{s}\right)\right]\mathrm{K}_{1/3}\left(z_q\right) \\ & - \frac{\omega^2}{2\varepsilon'\varepsilon}\int_{z_q}^{\infty}dx\,\mathrm{K}_{1/3}\left(x\right)\Big[\left(\vec{\zeta}_i\cdot\vec{s}\right)\left(\vec{\zeta}_f\cdot\vec{b}\right) \\ & + \left(\vec{\zeta}_i\cdot\vec{b}\right)\left(\vec{\zeta}_f\cdot\vec{s}\right)\Big]\Bigg\}, \end{aligned} \tag{4}$$

$$F_2 = -\frac{\alpha}{2\sqrt{3}\pi\gamma^2}\,d\omega\left\{\frac{\varepsilon^2-\varepsilon'^2}{2\varepsilon'\varepsilon}\mathrm{K}_{1/3}(z_q)\left[\vec{s}\cdot\left(\vec{\zeta}_f\times\vec{\zeta}_i\right)\right]\right.$$
$$+\left[-\frac{\varepsilon^2-\varepsilon'^2}{\varepsilon'\varepsilon}\mathrm{K}_{2/3}(z_q)+\frac{\omega}{\varepsilon}\int_{z_q}^{\infty}dx\,\mathrm{K}_{1/3}(x)\right]\left(\vec{\zeta}_i\cdot\vec{\nu}\right)$$
$$+\left[-\frac{\varepsilon^2-\varepsilon'^2}{\varepsilon'\varepsilon}\mathrm{K}_{2/3}(z_q)+\frac{\omega}{\varepsilon'}\int_{z_q}^{\infty}dx\,\mathrm{K}_{1/3}(x)\right]\left(\vec{\zeta}_f\cdot\vec{\nu}\right)$$
$$+\frac{\omega^2}{2\varepsilon'\varepsilon}\mathrm{K}_{1/3}(z_q)\left[\left(\vec{\zeta}_i\cdot\vec{\nu}\right)\left(\vec{\zeta}_f\cdot\vec{b}\right)\right.$$
$$\left.\left.+\left(\vec{\zeta}_i\cdot\vec{b}\right)\left(\vec{\zeta}_f\cdot\vec{\nu}\right)\right]\right\}, \tag{5}$$

$$F_3 = \frac{\alpha}{2\sqrt{3}\pi\gamma^2}d\omega\left\{\mathrm{K}_{2/3}(z_q)+\frac{\varepsilon^2+\varepsilon'^2}{2\varepsilon'\varepsilon}\mathrm{K}_{2/3}(z_q)\left(\vec{\zeta}_i\cdot\vec{\zeta}_f\right)\right.$$
$$-\left[\frac{\omega}{\varepsilon'}\left(\vec{\zeta}_i\cdot\vec{b}\right)+\frac{\omega}{\varepsilon}\left(\vec{\zeta}_f\cdot\vec{b}\right)\right]\mathrm{K}_{1/3}(z_q)$$
$$+\frac{\omega^2}{2\varepsilon'\varepsilon}\left[-\mathrm{K}_{2/3}(z_q)\left(\vec{\zeta}_i\cdot\vec{\nu}\right)\left(\vec{\zeta}_f\cdot\vec{\nu}\right)+\int_{z_q}^{\infty}dx\,\mathrm{K}_{1/3}(x)\right.$$
$$\left.\left.\times\left[\left(\vec{\zeta}_i\cdot\vec{b}\right)\left(\vec{\zeta}_f\cdot\vec{b}\right)-\left(\vec{\zeta}_i\cdot\vec{s}\right)\left(\vec{\zeta}_f\cdot\vec{s}\right)\right]\right]\right\}. \tag{6}$$

Here, $\vec{\nu}=\vec{v}/v$, $\vec{b}=\vec{\nu}\times\vec{s}$, $z_q=2\omega/(3\chi_e\varepsilon')$, ε and ε' are the energies of the emitting particle before and after emission, respectively, $\vec{\zeta}_i$ and $\vec{\zeta}_f$ are the spin vectors before and after emission, respectively, and ω is the emitted photon energy.

The emission probability and the polarization of the emitted photon both depend on the initial electron spin $\vec{\zeta}_i$. For instance, the emission probability is larger for the spin-down electrons, with respect to the magnetic field direction in the rest frame of the electron, than for the spin-up electrons, as shown in Fig. 1(a). The dependence of the polarization of the photon on $\vec{\zeta}_i$ is more remarkable, as shown in Fig. 1(b). For the low-energy region, the Stokes parameter $\xi_3 \sim 0.5$ regardless of the initial electron spin. However, with an increase in the energy of the emitted photons, ξ_3 increases to $\xi_3 = 1$ for the spin-up electrons, while it decreases to $\xi_3 = -1$ for the opposite case.

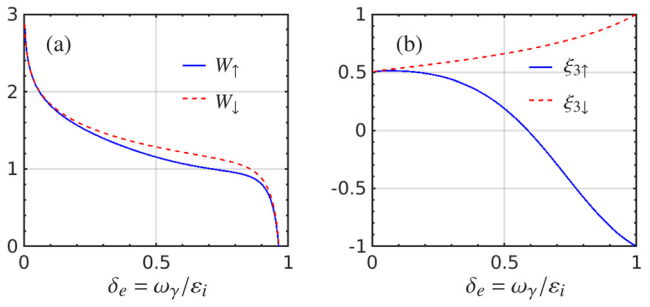

FIG. 1. (a) Photon emission probability $\log_{10} W_i$ (arbitrary units) and (b) Stokes parameter ξ_{3i} ($i \in \uparrow, \downarrow$) vs emitted photon energy $\delta_e = \omega_\gamma/\varepsilon_i$ for $\chi_e = 10$. i denotes the electron spin before the emission with respect to the magnetic field direction.

B. Photon-polarization-resolved pair production probabilities

Here, we provide the probability of polarized electron–positron pair production with a polarized photon. The polarization of the photon is defined as follows:

$$\vec{e} = a_1\vec{e}_1 + a_2\vec{e}_2, \tag{7}$$

$$\vec{e}_1 = \frac{\vec{E}-\vec{n}\left(\vec{n}\cdot\vec{E}\right)+\vec{n}\times\vec{B}}{\left|\vec{E}-\vec{n}\left(\vec{n}\cdot\vec{E}\right)+\vec{n}\times\vec{B}\right|}, \tag{8}$$

$$\vec{e}_2 = \vec{n}\times\vec{e}_1, \qquad \vec{n} = \frac{\vec{k}}{|\vec{k}|}. \tag{9}$$

The pair production rate of the polarized photon takes the form

$$dW_p = \frac{1}{2}\left(dW^{(11)}+dW^{(22)}\right)+\frac{1}{2}\xi_1\left(dW^{(11)}-dW^{(22)}\right)$$
$$-i\frac{1}{2}\xi_2\left(dW^{(21)}-dW^{(12)}\right)+\frac{1}{2}\xi_3\left(dW^{(11)}-dW^{(22)}\right)$$
$$=\frac{1}{2}\left(G_0+\xi_1G_1+\xi_2G_2+\xi_3G_3\right), \tag{10}$$

where $\xi_i = G_i/G_0$ ($i = 1, 2, 3$) are the Stokes parameters, and

$$G_0 = \frac{\alpha m^2 d\varepsilon}{2\sqrt{3}\pi\omega^2}\left\{\left[\int_{z_p}^{\infty}dx\,\mathrm{K}_{1/3}(x)+\frac{\varepsilon_+^2+\varepsilon^2}{\varepsilon_+\varepsilon}\mathrm{K}_{2/3}(z_p)\right]\right.$$
$$+\left[\int_{z_p}^{\infty}dx\,\mathrm{K}_{1/3}(x)-2\mathrm{K}_{2/3}(z_p)\right]\left(\vec{\zeta}_-\cdot\vec{\zeta}_+\right)$$
$$+\left[\frac{\omega}{\varepsilon_+}\left(\vec{\zeta}_+\cdot\vec{b}\right)-\frac{\omega}{\varepsilon}\left(\vec{\zeta}_-\cdot\vec{b}\right)\right]\mathrm{K}_{1/3}(z_p)$$
$$+\left[\frac{\varepsilon_+^2+\varepsilon^2}{\varepsilon\varepsilon_+}\int_{z_p}^{\infty}dx\,\mathrm{K}_{1/3}(x)\right.$$
$$\left.\left.-\frac{(\varepsilon_+-\varepsilon)^2}{\varepsilon\varepsilon_+}\mathrm{K}_{2/3}(z_p)\right]\left(\vec{\zeta}_-\cdot\vec{\nu}\right)\left(\vec{\zeta}_+\cdot\vec{\nu}\right)\right\}, \tag{11}$$

$$G_1 = \frac{\alpha m^2 d\varepsilon}{2\sqrt{3}\pi\omega^2}\left\{-\frac{\varepsilon_+^2-\varepsilon^2}{2\varepsilon_+\varepsilon}\mathrm{K}_{2/3}(z_p)\left[\vec{\nu}\cdot\left(\vec{\zeta}_+\times\vec{\zeta}_-\right)\right]\right.$$
$$+\left[\frac{\omega}{\varepsilon}\left(\vec{\zeta}_+\cdot\vec{s}\right)-\frac{\omega}{\varepsilon_+}\left(\vec{\zeta}_-\cdot\vec{s}\right)\right]\mathrm{K}_{1/3}(z_p)$$
$$-\frac{\omega^2}{2\varepsilon_+\varepsilon}\int_{z_p}^{\infty}dx\,\mathrm{K}_{1/3}(x)\left[\left(\vec{\zeta}_-\cdot\vec{b}\right)\left(\vec{\zeta}_+\cdot\vec{s}\right)\right.$$
$$\left.\left.+\left(\vec{\zeta}_-\cdot\vec{s}\right)\left(\vec{\zeta}_+\cdot\vec{b}\right)\right]\right\}, \tag{12}$$

$$G_2 = \frac{\alpha m^2 d\varepsilon}{2\sqrt{3}\pi\omega^2}\left\{-\frac{\omega^2}{2\varepsilon_+\varepsilon}\mathrm{K}_{1/3}(z_p)\left[\vec{s}\cdot\left(\vec{\zeta}_-\times\vec{\zeta}_+\right)\right]\right.$$
$$+\left[\frac{\omega}{\varepsilon_+}\int_{z_p}^{\infty}dx\,\mathrm{K}_{1/3}(x)+\frac{\varepsilon_+^2-\varepsilon^2}{\varepsilon_+\varepsilon}\mathrm{K}_{2/3}(z_p)\right]\left(\vec{\zeta}_+\cdot\vec{\nu}\right)$$
$$+\left[\frac{\omega}{\varepsilon}\int_{z_p}^{\infty}dx\,\mathrm{K}_{1/3}(x)-\frac{\varepsilon_+^2-\varepsilon^2}{\varepsilon_+\varepsilon}\mathrm{K}_{2/3}(z_p)\right]\left(\vec{\zeta}_-\cdot\vec{\nu}\right)$$
$$-\frac{\varepsilon_+^2-\varepsilon^2}{2\varepsilon_+\varepsilon}\mathrm{K}_{1/3}(z_p)\left[\left(\vec{\zeta}_-\cdot\vec{\nu}\right)\left(\vec{\zeta}_+\cdot\vec{b}\right)\right.$$
$$\left.\left.+\left(\vec{\zeta}_-\cdot\vec{b}\right)\left(\vec{\zeta}_+\cdot\vec{\nu}\right)\right]\right\}, \tag{13}$$

$$G_3 = \frac{\alpha m^2 d\varepsilon}{2\sqrt{3}\pi\omega^2}\left\{-\mathrm{K}_{2/3}(z_p)+\frac{\varepsilon_+^2+\varepsilon^2}{2\varepsilon_+\varepsilon}\mathrm{K}_{2/3}(z_p)\left(\vec{\zeta}_-\cdot\vec{\zeta}_+\right)\right.$$
$$+\left[-\frac{\omega}{\varepsilon}\left(\vec{\zeta}_+\vec{b}\right)+\frac{\omega}{\varepsilon_+}\left(\vec{\zeta}_-\vec{b}\right)\right]\mathrm{K}_{1/3}(z_p)$$
$$-\frac{(\varepsilon_+-\varepsilon)^2}{2\varepsilon_+\varepsilon}\mathrm{K}_{2/3}(z_p)\left(\vec{\zeta}_-\cdot\vec{\nu}\right)\left(\vec{\zeta}_+\cdot\vec{\nu}\right)$$
$$+\frac{\omega^2}{2\varepsilon_+\varepsilon}\int_{z_p}^{\infty}dx\,\mathrm{K}_{1/3}(x)\left[\left(\vec{\zeta}_-\cdot\vec{b}\right)\left(\vec{\zeta}_+\cdot\vec{b}\right)\right.$$
$$\left.\left.-\left(\vec{\zeta}_-\cdot\vec{s}\right)\left(\vec{\zeta}_+\cdot\vec{s}\right)\right]\right\}. \tag{14}$$

Here, $\vec{\nu}=\vec{v}/v$ is the velocity direction of the produced pairs, which satisfies $\vec{\nu}_-\approx\vec{\nu}_+\approx\vec{n}$ in the relativistic case, $\vec{s}=\vec{w}/|\vec{w}|$ is the acceleration direction of the produced particles, and $\vec{b}=\vec{\nu}\times\vec{s}$ is the magnetic field direction in the rest frame of the electron/positron. The parameter $z_p=2\omega/(3\chi_\gamma\varepsilon\varepsilon_+)$, where ω, ε, and ε_+ are the energies of the parent photon and the produced electron and positron, respectively, and the quantum strong-field parameter $\chi_\gamma=|e|\sqrt{\left(F_{\mu\nu}k^\nu\right)^2}/m^3$, with $F_{\mu\nu}$ and k^ν being the electromagnetic field strength tensor and the photon momentum four-vector, respectively. Averaging over the photon polarization yields the spin-resolved pair production probability[44,56,57] $dW_p(0)=\frac{1}{2}G_0$.

Summing over the final spin states of the electron, one can obtain the polarization of the positron depending on the photon polarization:[25,44]

$$\vec{\zeta}_+^{\,f,\xi}=\frac{\xi_1 f_3\frac{\omega}{\varepsilon}\vec{s}+\xi_2\vec{\nu}\left(\frac{\omega}{\varepsilon_+}f_1+\frac{\varepsilon_+^2-\varepsilon^2}{\varepsilon\varepsilon_+}f_2\right)+\left(\frac{\omega}{\varepsilon_+}-\xi_3\frac{\omega}{\varepsilon}\right)\vec{b}\,f_3}{f_1+\frac{\varepsilon^2+\varepsilon_+^2}{\varepsilon\varepsilon_+}f_2-\xi_3 f_2}. \tag{15}$$

In the case of an unpolarized photon,[23]

$$\vec{\zeta}_+^{\,f,0}=\frac{\frac{\omega}{\varepsilon_+}\vec{b}\,f_3}{f_1+\frac{\varepsilon^2+\varepsilon_+^2}{\varepsilon\varepsilon_+}f_2}, \tag{16}$$

where $f_1=\int_{z_p}^{\infty}dx\,\mathrm{K}_{1/3}(x)$, and $f_2=\mathrm{K}_{2/3}(z_p)$, $f_3=\mathrm{K}_{1/3}(z_p)$. Equations (15) and (16) show that the photon polarization has significant effects on the positron polarization $\vec{\zeta}_+^{\,f}$. The longitudinal polarization of positrons is completely missing if the photon polarization is averaged over, while the transverse polarization either increases or decreases, as determined by ξ_1 and ξ_3.

The correlation of the electron and positron polarizations in the pair production is analyzed in Fig. 2. In the case $\xi_1=\xi_2=0$ and $\xi_3>0$, the probabilities of e^+e^- co-polarization are higher than those of counter-polarization with respect to the magnetic field direction, i.e., $dW_{\uparrow\uparrow}$, $dW_{\downarrow\downarrow}>dW_{\downarrow\uparrow}$, $dW_{\uparrow\downarrow}$, as shown in Fig. 2(a). On the other hand, when $\xi_3<0$, the probability of producing an electron with spin down and a positron with spin up dominates, i.e., $dW_{\downarrow\uparrow}>dW_{\downarrow\downarrow}$, $dW_{\uparrow\uparrow}$, $dW_{\uparrow\downarrow}$, as shown in Fig. 2(b).

After integration over the electron spin, one obtains the dependence of the positron spin on the positron energy and the polarization of the parent photon, as shown in Fig. 2(c). For $\xi_3<0$, the positron polarization degree decreases gradually with increasing positron energy. The domination of $dW_{\downarrow\uparrow}$ results in a high polarization degree of positrons with spin up through the whole spectrum. For a photon with $\xi_3>0$, the polarization of the produced positron

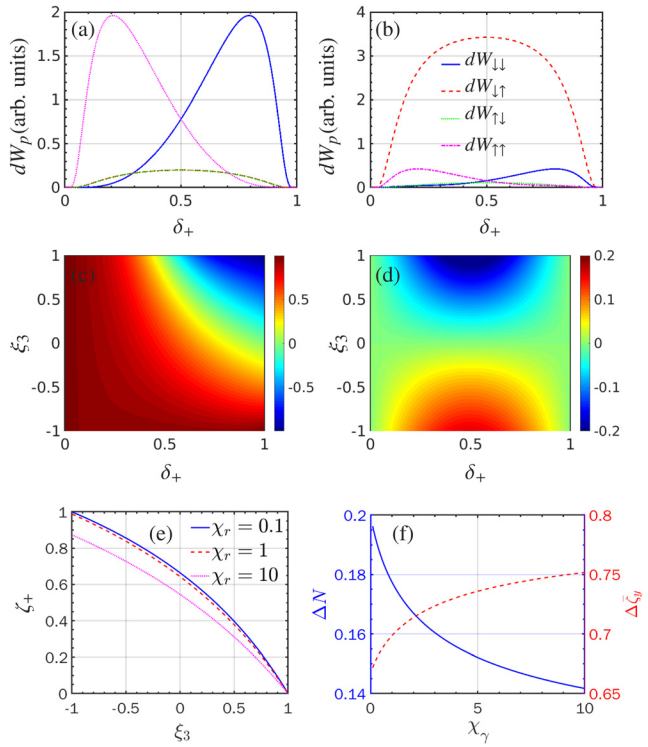

FIG. 2. (a) and (b) Pair production probability $dW_{\zeta_-\zeta_+}$ for a polarized photon with (a) $\xi_1=\xi_2=0$, $\xi_3=1$ and (b) $\xi_3=-1$. (c) Positron polarization $\zeta_+=\sum_{\zeta_-}\frac{dW_{\zeta_-\uparrow}-dW_{\zeta_-\downarrow}}{dW_{\zeta_-\uparrow}+dW_{\zeta_-\downarrow}}$ vs ξ_3 and δ_+. In (a)–(c), $\chi_\gamma=3$. (d) Ratio of the photon-polarization-resolved and averaged pair production probabilities $\frac{dW_p(\xi)-dW_p(0)}{dW_p(\xi)+dW_p(0)}$ vs ξ_3 and δ_+. (e) $\overline{\zeta}_+=\frac{\sum_i\zeta_+(\delta_i)dW_p(\delta_i)}{\sum_i dW_p(\delta_i)}$ vs ξ_3 for $\chi_\gamma=0.1$ (blue solid curve), 1 (red dashed curve), and 10 (magenta dotted curve). (f) Relative differences $\Delta N=[N(0)-N(\xi)]/N(\xi)$ (solid curve) and $\Delta\zeta_y=[\zeta_y^+(0)-\zeta_y^+(\xi)]/\zeta_y^+(\xi)$ (dashed curve) vs χ_γ for $\xi_3=0.5$.

decreases dramatically to a negative value with increasing energy, resulting in a smaller averaged polarization compared with the case of $\xi_3 = 0$. In particular, when $\xi_3 \sim 1$, as shown in Fig. 2(a), the probability $\sum_{\zeta_-} dW_{\zeta_-\uparrow} \approx \sum_{\zeta_-} dW_{\zeta_-\downarrow}$. The polarizations of positrons in high-energy ($\delta_+ > 0$) and low-energy ($\delta_+ < 0$) regions cancel each other, producing unpolarized positrons after energy integration. Therefore, if the parent photon is polarized along the laser polarization direction, i.e., $\xi_3 = 1$, then the produced pairs are unpolarized. However, if the polarization of the parent photon is orthogonal to the laser polarization, i.e., $\xi_3 = -1$, the produced pairs have a high degree of polarization, with positrons spin-up and electrons spin-down. After integration over the positron energy, one obtains the relation between the positron polarization and that of its parent photon, as shown in Fig. 2(e). The polarization of the positron decreases monotonically with increasing ξ_3, which provides a way of estimating the polarization of the intermediate photons during nonlinear Compton scattering. For instance, if the polarization of positrons is measured to be 37% at $\chi_\gamma = 1$, then the polarization of the intermediate photons is around $\xi_3 = 0.5$. The dependences of the relative differences ΔN and $\Delta\zeta_y$ on χ_γ are shown in Fig. 2(f). For $\xi_3 = 0.5$, the relative difference in positron number ΔN decreases with increasing χ_γ, while the relative difference in positron polarization $\Delta\zeta_y$ increases with χ_γ increases.

The photon polarization affects not only the polarization of produced pairs, but also the pair density, as shown in Fig. 2(d). When $\xi_3 > 0$, the pair production probability is smaller than in the case where photon polarization is unresolved, i.e., $\xi_3 = 0$. In contrast, photons with $\xi_3 < 0$ yield more pairs than unpolarized photons.

C. Stochastic algorithm

To simulate the nonlinear Compton scattering of a strong laser pulse at an ultrarelativistic electron beam, we modified the three-dimensional Monte Carlo method[25] by employing the fully polarization-resolved pair production probabilities given in Sec. II B. The developed Monte-Carlo method includes the correlation of electron and positron spins, providing a complete description of polarization effects in strong-field QED processes. In each simulation step, one calculates the total emission rate to determine the occurrence of photon emission and the pair production rate to determine the pair production event, using a common QED Monte Carlo stochastic algorithm.[41–43] The spins of electron/positron after emission and creation are determined by the polarization-resolved emission probability of Sec. II A and the pair production probability of Sec. II B, respectively, according to the stochastic algorithm. The electron/positron spin instantaneously collapses into one of its basis states defined with respect to the instantaneous spin quantization axis (SQA), which is chosen according to the properties of the scattering process. Moreover, since the probability of no emission is also polarization-resolved and asymmetric along an arbitrary SQA, it is necessary to include the spin variation between emissions induced by radiative polarization, as well as the spin precession governed by the Thomas–Bargmann–Michel–Telegdi equation;[58–60] for more details, see Ref. 25. The polarization of the emitted photon is determined using a similar stochastic procedure, which has also been used in laser–plasma simulation codes.[61]

III. SIMULATION RESULT

Recently, various schemes have been proposed to produce transversely polarized positrons via strong lasers, but these have neglected photon polarization. Here, we proceed to investigate photon polarization effects on the transverse polarization of positrons with the fully polarization-resolved Monte Carlo method, and compare the result with that obtained using the unpolarized photon model.

A PW laser with intensity $\xi_0 = |e|E_0/m\omega = 100$ ($I = 10^{22}$ W/cm^2) counterpropagates with a relativistic electron beam with an energy of $\varepsilon_0 = 10$ GeV, with the setup shown in Fig. 3. The wavelength of the laser is $\lambda_0 = 1$ μm, the beam waist size $w = 5\lambda_0$, the pulse duration $\tau_p = 8$ T, and the ellipticity $\varepsilon = 0.03$. The electron beam consists of $N_e = 6 \times 10^6$ electrons, with the beam length $L_e = 5\lambda_0$, beam radius $r_e = \lambda_0$, energy divergence $\Delta\varepsilon = 0.06$, and angular divergences $\Delta\theta = 0.3$ mrad and $\Delta\phi = 1$ mrad. The initial electron beam is fully polarized along the y direction.

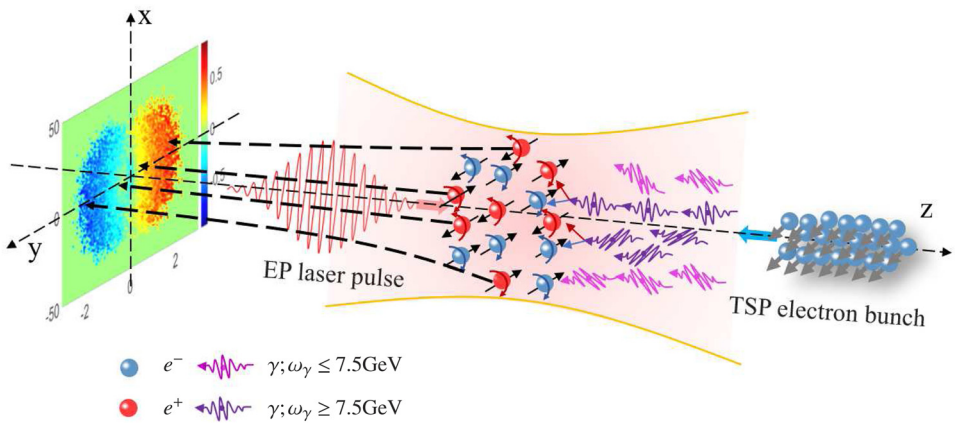

FIG. 3. Scheme for producing polarized positrons via nonlinear Compton scattering of an initially transversely polarized electron off a strong elliptically polarized laser pulse. The energetic gamma photons in the region $\theta_y^\gamma < 0$ have high polarizations up to $\xi_3 = 1$, resulting in a reduction in or even reversal of polarization of positrons as θ_y^+ decreases.

The impact of the photon polarization on pair production is elucidated in Fig. 4. The positron density decreases when the photon polarization is resolved in both photon emission and pair production processes, as shown in Figs. 3(a), 3(c), and 3(e). The difference in positron density between using a polarization-resolved or unresolved treatment is approximately $(N(0) - N(\xi))/N(\xi) \approx 12.6\%$. More importantly, the y component of polarization $\bar{\zeta}_y$ decreases dramatically at small angles, even showing a reversal of polarization direction [see Fig. 4(d)]. As a consequence, the symmetric angular distribution of $\bar{\zeta}_y$ near $\theta_y = 0$ is distorted when the intermediate photon polarization is considered, as shown in Fig. 4(f). The angular distribution of $\bar{\zeta}_y$ oscillates around the small-angle region, instead of exhibiting a monotonic increase as in the photon-polarization-averaged case. The average polarization of the positron beam decreases by $[\bar{\zeta}_y(0) - \bar{\zeta}_y(\xi)]/\bar{\zeta}_y(\xi) \approx 35\%$.

To understand the effects of photon polarization on pair production, we investigate the polarization of emitted photons in $\theta_y^\gamma > 0$ and $\theta_y^\gamma < 0$ separately, as shown in Fig. 5. The photon density emitted within the angular region $\theta_y^\gamma < 0$ is larger than within the region $\theta_y^\gamma > 0$, especially in the high-energy region, as shown in Fig. 5(a). When an electron with $\vec{\zeta}_i = \vec{b}$ counterpropagates to the laser field, the direction of the instantaneous quantization axis is $\vec{n} = \vec{\zeta}^f/|\vec{\zeta}^f|$,[25] with

$$\vec{\zeta}^f = \frac{(2f_2 - f_1)\vec{\zeta}_i - \frac{\omega}{\varepsilon'}\vec{b}\,f_3 + \frac{\omega}{\varepsilon'\varepsilon}(f_2 - f_1)\left(\vec{\zeta}_i \cdot \vec{\hat{\nu}}\right)\vec{\hat{\nu}}}{\frac{\varepsilon^2 + \varepsilon'^2}{\varepsilon'\varepsilon}f_2 - f_1 - \frac{\omega}{\varepsilon}\vec{\zeta}_i \cdot \vec{b}\,f_3}, \quad (17)$$

which is mostly along B_y and changes sign every half-cycle. For an electron with initial spin $\zeta_y = 1$, its spin is parallel (spin-up) and antiparallel (spin-down) to the quantization axis in the half-cycles with $B_y > 0$ and $B_y < 0$, respectively. The emission probability is larger when the electron is spin-down before the emission, as shown in Fig. 5(a), which is in accordance with the analysis of the spin-resolved probability given in Fig. 1(a). Further, the photon emission direction is parallel to the momentum of the emitting particle, and the photons emitted when $B_y > 0$ and $B_y < 0$ propagate with $p_y < 0$ and $p_y > 0$, respectively, because the oscillation phase of p_y has a π delay with respect to B_y. Therefore, the electrons emit photons with $\theta_y^\gamma > 0$ at $B_y > 0$ and photons with $\theta_y^\gamma < 0$ at $B_y < 0$. The latter case has a higher emitted photon number than the former, owing to the larger emission probability $W_{r\downarrow} > W_{r\uparrow}$, as explained above. More importantly, the electrons with spin up (spin down) have a higher probability to emit photons with $-1 < \xi_3 < 0.5$ ($0.5 < \xi_3 < 1$). Therefore, the radiation with $\theta_y > 0$ comes mainly from photon emission at $B_y > 0$, and has polarization $-1 < \xi_3 < 0.5$, while the radiation with $\theta_y < 0$ comes from photon emission at $B_y < 0$, which has polarization $0.5 < \xi_3 < 1$, as shown in Fig. 5(b).

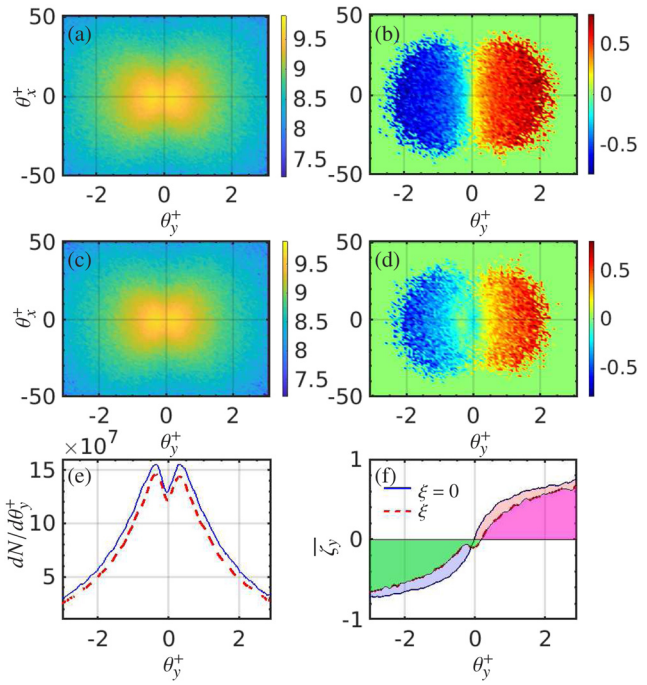

FIG. 4. (a) Polarized positron density distribution $d^2N^+/d\theta_x^+ d\theta_y^+$ (rad^{-2}) and (b) averaged polarization degree of y component ζ_y vs $\theta_x^+ = p_x/p_z$ (rad) and $\theta_y^+ = p_y/p_z$ (rad) for photon-polarization-unresolved pair production. (c) and (d) Corresponding plots for photon-polarization-resolved pair production. (e) Polarized positron density distribution $dN/d\theta_y$ (rad^{-1}) vs θ_y^+ (rad) for unresolved (solid curve) and resolved (dashed curve) photon polarization. (f) Averaged polarization degree ζ_y vs θ_y^+ (rad) for unresolved (solid curve) and resolved (dashed curve) photon polarization.

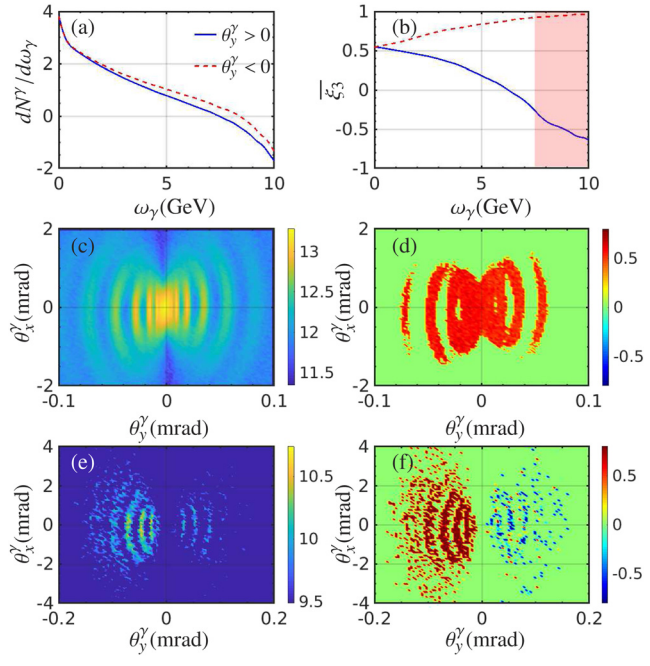

FIG. 5. (a) and (b) $\log_{10} dN^\gamma/d\omega_\gamma$ and averaged Stokes parameter ξ_3, respectively, of gamma photons emitted in $\theta_y^\gamma > 0$ (solid line) and $\theta_y^\gamma < 0$ (dashed line) vs photon energy ω_γ in $|\theta_x|, |\theta_y| < 10$ mrad. (c) and (d) Angular distributions of $d^2N^\gamma/d\theta_x^\gamma d\theta_y^\gamma$ (rad^{-2}) and ξ_3, respectively, vs $\theta_x^\gamma = k_x/k_z$ and $\theta_y^\gamma = k_y/k_z$. (e) and (f) Angular distributions of $d^2N^\gamma/d\theta_x^\gamma d\theta_y^\gamma$ (rad^{-2}) and ξ_3, respectively, for photons with energy $\varepsilon > 7.5$ GeV [shaded red in (b)].

The fringes in the angular distribution seen in Figs. 5(c)–5(e) are due to the radiation in different laser cycles. As shown in Fig. 5(b), $\bar{\xi}_3$ in the high-energy region is positive for spin-down electrons and negative for spin-up electrons. However, since the radiation is dominated by low-energy photons with $\xi_3 \sim 0.51$, the angular distribution of the photon polarization in Fig. 5(d) is also dominated by $\xi_3 \sim 0.51$. Nevertheless, the low-energy emissions have been filtered, a correlation of photon polarization and emission angle can be seen in Figs. 4(e) and 4(f). As expected, the photons distributed in $\theta_y^\gamma < 0$ have $\bar{\xi}_3 < 0$, while in the region $\theta_y^\gamma < 0$, the polarization is $\bar{\xi}_3 > 0$. Since the pairs are produced mostly by energetic photons, the distinct polarization properties of high-energy photons in $\theta_y^\gamma < 0$ and $\theta_y^\gamma > 0$ break the symmetry of the angular distribution of polarization.

The separation of positron polarization along the propagation direction can be explained,[32] taking into account that the final momentum of the created electron (positron) is determined by the laser vector potential $A_y(t_p)$ at the instant of creation t_p: $p_f = p_i + eA_y(t_p)$, where p_i is the momentum inherited from the parent photon, with vanishing average value $\bar{p}_i = 0$. On the other hand, when the photon is linearly polarized with $(0, 0, \xi_3)$, the SQA for pair production of such a photon is along the laser magnetic field direction, $\vec{n} = \vec{\zeta}_+^{f,\xi}/|\vec{\zeta}_+^{f,\xi}| = \vec{b}$. Therefore, the positrons produced at $A_y(t_p) < 0$ acquire a final momentum $p_f \approx eA_y(t_p) > 0$ and are polarized along $\zeta_y > 0$, since the instantaneous SQA is along $y > 0$ at t_p. Similarly, one has $\zeta_y < 0$ when $p_f < 0$.

To reveal the origin of the abnormal polarization features in the small-angle region, we artificially turn on pair production of photons with $\theta_y^\gamma > 0$ and $\theta_y^\gamma < 0$ separately. As shown in Fig. 5(b), the photons with $\theta_y^\gamma < 0$ have $\xi_3 \sim 1$ at the high-energy end of the spectrum. These hard photons have a higher probability of producing energetic positrons antiparallel with the magnetic field, as discussed in Sec. II B, resulting in a reversed polarization direction in the small-angle region and an overall decrease in the averaged polarization of positrons, as shown in Fig. 6(b). Moreover, since the parent photon with $\theta_y^\gamma < 0$ has $\bar{p}_i < 0$, the positron distribution is slightly shifted toward $\theta_y^+ < 0$. Meanwhile, the polarization of hard photons at the $\theta_y^\gamma > 0$ side reaches $\xi_3 \sim -1$ [Fig. 5(b)]. If these photons are collected to produce pairs, highly polarized positrons could be obtained owing to the overwhelming dominance of the spin-up positrons, $dW_{\downarrow\uparrow}(\xi_3 = -1) \gg dW_{\downarrow\uparrow}(\xi_3 = 0)$. In the present case, the $\bar{\zeta}_y$ of positrons produced by photons with $\theta_y^\gamma > 0$ increases monotonically with θ_y^+, and the angular distribution shifts slightly toward $\theta_y^+ > 0$. The pair production probability is inversely proportional to ξ_3, and the photons with $\theta_y^\gamma < 0$ have larger $\bar{\xi}_3$ than those with $\theta_y^\gamma > 0$, and therefore more positrons are produced at $\theta_y^\gamma > 0$, as shown in Fig. 6(a). Thus, the domination of pair production of photons in $\theta_y^\gamma < 0$ and $\bar{p}_i < 0$ results in a decrease in the polarization of the positron beam and an asymmetric angular distribution of polarization.

When the initial electrons are unpolarized as in Ref. 23, the photons are equally distributed in $\theta_y^\gamma > 0$ and $\theta_y^\gamma < 0$, with polarization $\bar{\xi}_3 \approx 0.51\%$, as shown in Figs. 7(a) and 7(b). Consequently, the abnormal polarization feature in the small-angle region vanishes because of a lack of angle-dependent photon polarization with $\xi_3 \sim 1$. As shown in Figs. 7(c) and 7(d), the produced positrons have a symmetric angular distribution of polarization. On the other hand, the positron density and average polarization decrease when the photon polarization is resolved, regardless of the spin of the initial electrons, as also shown in Figs. 7(c) and 7(d). The difference in positron density between using a polarization-resolved or unresolved treatment is approximately $\Delta N = [N(\xi) - N(0)]/N(\xi) \approx 12\%$, and the difference in polarization is $\Delta\bar{\zeta}_y = [\bar{\zeta}_y(\xi) - \bar{\zeta}_y(0)]/\bar{\zeta}_y(\xi) \approx 34\%$, both of , which are close to the values obtained with our scheme, namely, $\Delta N \approx 13\%$ and $\Delta\bar{\zeta}_y \approx 35\%$. This is because the photons emitted are polarized with $\bar{\xi}_3 \approx 0.51$, regardless of the initial spin of the electrons. Specifically, since the photon polarization reads[13]

$$\xi_3 = \frac{f_2 - \frac{\omega}{\varepsilon'}\left(\vec{\zeta}_i \cdot \vec{b}\right) f_3}{-f_1 + \frac{\varepsilon^2 + \varepsilon'^2}{\varepsilon\varepsilon'} f_2 - \frac{\omega}{\varepsilon}\left(\vec{\zeta}_i \cdot \vec{b}\right) f_3}, \tag{18}$$

and

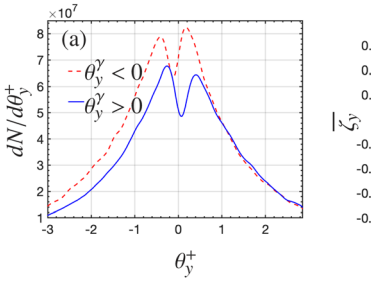

FIG. 6. (a) Polarized-positron density distribution $dN/d\theta_y^+$ (rad^{-1}) and (b) averaged polarization degree ζ_y vs positron polar angle θ_y^+ (rad) for positrons produced by photons with $\theta_y^\gamma > 0$ (solid curves) and $\theta_y^\gamma < 0$ (dashed curves).

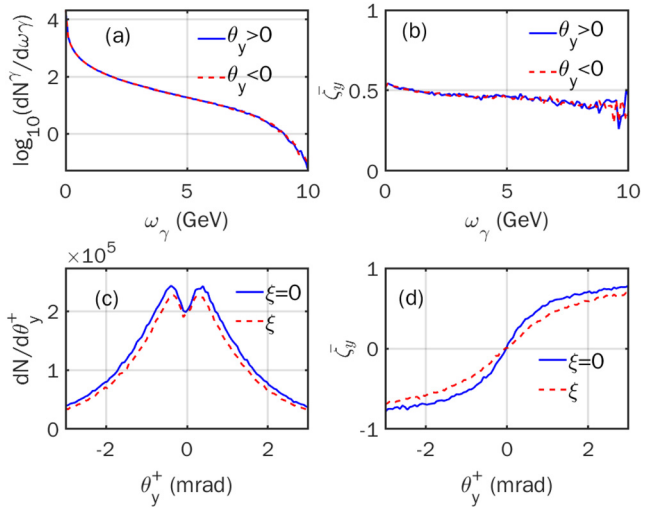

FIG. 7. (a) and (b) $\log_{10} dN^\gamma/d\omega_\gamma$ and averaged Stokes parameter ξ_3, respectively, of gamma photons emitted in $\theta_y^\gamma > 0$ (solid curves) and $\theta_y^\gamma < 0$ (dashed curves) vs photon energy ω_γ in $|\theta_x|, |\theta_y| < 10$ mrad. (c) and (d) Polarized positron density distribution $dN/d\theta_y$ (mrad^{-1}) and averaged polarization degree ζ_y, respectively, vs θ_y (mrad) for unresolved (dashed curves) and resolved (solid curves) photon polarization.

$$-f_1+\frac{\varepsilon^2+\varepsilon'^2}{\varepsilon\varepsilon'}f_2\ll\frac{\omega}{\varepsilon}f_3 \tag{19}$$

for most emitted photons, the average polarization

$$\bar{\xi}_3\left(\vec{\zeta}_i\right)\approx\bar{\xi}_3(0)=f_2\Big/\left(-f_1+\frac{\varepsilon^2+\varepsilon'^2}{\varepsilon\varepsilon'}f_2\right)\approx 0.51, \tag{20}$$

owing to the change in sign of the term $\vec{\zeta}_i\cdot\vec{b}$ as the field oscillates. Therefore, the initial electron spin is not important for density/polarization decrease, but essential for polarization features in the small-angle region, which could be used as additional information for detecting photon polarization.

With experimental feasibility in mind, it is interesting to find how ΔN and $\Delta\bar{\zeta}_y$ depend on the laser parameters. The produced positron number $N^+\propto N_\gamma\chi_\gamma\tau_p$, where N_γ is the gamma-photon number and $\chi_\gamma\propto a_0\varepsilon_0$ is the quantum strong-field parameter. Thus, N^+ increases with increasing a_0 and τ_p, as shown in Figs. 8(a) and 8(c). Moreover, since the relative difference ΔN is inversely proportional to χ_γ, as shown in Fig. 2(f), ΔN decreases as a_0 increases, owing to the increase in χ_γ. On the other hand, since the χ_γ barely changes with τ_p, the variation of ΔN is negligible in Fig. 8(c). Meanwhile, $\Delta\bar{\zeta}_y$ of the produced positrons increases with χ_γ, as shown in Fig. 2(f). However, the positron polarization decreases after the instant of creation t_i, owing to further radiative polarization in the laser field, which affects the scaling law of $\Delta\bar{\zeta}_y$. The time evolution of the positron polarization due to radiative polarization is given by[62]

$$\bar{\zeta}_y(t)\propto\bar{\zeta}_y(t_i)e^{-\Psi_1(\chi_e)t}, \tag{21}$$

with

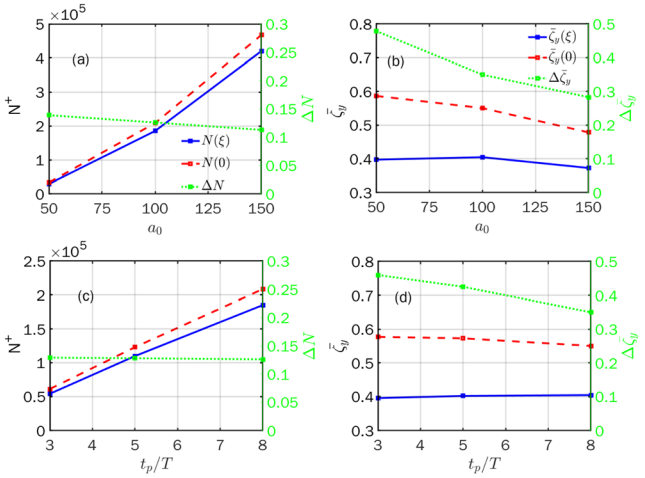

FIG. 8. (a) and (c) Positron number N^+ in the case of unresolved photon polarization (dashed lines) and in the resolved case (solid lines) and their relative difference ΔN (dotted lines) vs laser intensity a_0 (at $a_0=50$, 100, and 150) and laser pulse duration t_p (at $t_p=3$, 5, and 8 T), respectively. (b) and (d) Positron polarization $\bar{\zeta}_y$ in the case of unresolved photon polarization (dashed lines) and in the resolved case (solid lines) and their relative difference $\Delta\bar{\zeta}_y$ (dotted lines) vs laser intensity a_0 (at $a_0=50$, 100, and 150) and laser pulse duration t_p (at $t_p=3$, 5, and 8 T), respectively. Other parameters are the same as in Fig. 4.

$$\Psi_1(\chi_e)=\int_0^\infty\frac{u^2\,du}{(1+u)^3}\mathrm{K}_{2/3}\left(\frac{2}{3}\frac{u}{\chi_e}\right), \tag{22}$$

where $u=\omega/(\varepsilon_0-\omega)$. Therefore, the decrease in $\bar{\zeta}_y$ is proportional to $\bar{\zeta}_y(t_i)$, χ_e, and the interaction time t_f-t_i. As the laser intensity increases, the decrease in polarization is more dramatic, owing to the increase in χ_e, as shown in Fig. 8(b). Since the $\bar{\zeta}_y(t_i)$ is larger in the case of unresolved photon polarization than in the resolved case, the rate of reduction rate in the former is larger than in the later. Therefore, $\Delta\zeta_y$ decreases as a_0 increases. Similarly, as the laser pulse duration increases, the final polarization decreases, owing to enhancement of the radiative polarization. This effect is more noticeable in the case of unresolved photon polarization, owing to the higher $\bar{\zeta}_y(t_i)$, and therefore $\Delta\zeta_y$ is smaller for longer laser pulses.

IV. CONCLUSION

We have investigated the effects of photon polarization on pair production in the nonlinear Breit–Wheeler process via a newly developed Monte Carlo method employing fully polarization resolved quantum probabilities. We have shown that the longitudinal polarization of the produced positrons is induced solely by the photon polarization, while their transverse polarization can increase, decrease, or even be unchanged, depending on the polarization of the intermediate gamma photons. For the interaction of initially transversely polarized electrons and an elliptically polarized laser, both the polarization degree and density of the positrons are reduced when the polarization of the intermediate photons is taken into account. This is because the photons emitted during the nonlinear Compton process are partially polarized along the electric field direction, with $\bar{\xi}_3\approx0.51$. The hard photons in the angular region $\theta_y^\gamma<0$ have even higher polarization $\bar{\xi}_3\sim1$, causing the energetic positrons produced in the small-angle region to reverse the polarization direction. If one separates the intermediate hard gamma photons within $\theta_y^\gamma>0$, the polarization of positrons will be greatly enhanced owing to the dominance of $dW_{\downarrow\uparrow}$ probabilities throughout the spectrum. Our results confirm the important role of the intermediate photon polarization during strong-field QED processes and should be taken into account in the design and optimization of practical laser-driven polarized positron sources. Moreover, measurement of positron polarization in pair production processes can shed light on the intermediate interaction dynamics, particularly on the polarization properties of intermediate photons.

ACKNOWLEDGMENTS

This work was supported by the National Natural Science Foundation of China (Grants No. 12074262) and the Program for Professor of Special Appointment (Eastern Scholar) at Shanghai Institutions of Higher Learning and the Shanghai Rising-Star Program.

AUTHOR DECLARATIONS

Conflict of Interest

We have no conflicts of interest to disclose.

DATA AVAILABILITY

The data that support the findings of this study are available from the corresponding author [Y.-Y. Chen], upon reasonable request.

REFERENCES

[1]E. Voutier, "Physics perspectives at JLab with a polarized positron beam," EPJ Web of Conferences 73, (2014).

[2]Q. Collaboration *et al.*, "First determination of the weak charge of the proton," Phys. Rev. Lett. **111**, 141803 (2013).

[3]B. A. Mecking, G. Adams, S. Ahmad, E. Anciant, M. Anghinolfi, B. Asavapibhop, G. Asryan, G. Audit, T. Auger, H. Avakian *et al.*, "The CEBAF large acceptance spectrometer (CLAS)," Nucl. Instrum. Methods Phys. Res., Sect. A **503**, 513–553 (2003).

[4]A. Sokolov and I. Ternov, "On polarization and spin effects in the theory of synchrotron radiation," Sov. Phys.-Dokl. **8**, 1203–1205 (1964).

[5]I. M. Ternov, "Synchrotron radiation," Phys.-Usp. **38**, 409 (1995).

[6]V. N. Baier and V. M. Katkov, "Radiational polarization of electrons in inhomogeneous magnetic field," Phys. Lett. A **24**, 327–329 (1967).

[7]V. Baier, "Radiative polarization of electrons in storage rings," Sov. Phys.-Dokl. **14**, 695 (1972).

[8]Y. S. Derbenev, and A. Kondratenko, "Polarization kinetics of particles in storage rings," Sov. Phys.-JETP **37**, 968 (1973).

[9]I. Sakai, T. Aoki, K. Dobashi, M. Fukuda, A. Higurashi, T. Hirose, T. Iimura, Y. Kurihara, T. Okugi, T. Omori *et al.*, "Production of high brightness γ rays through backscattering of laser photons on high-energy electrons," Phys. Rev. Spec. Top.-Accel. Beams **6**, 091001 (2003).

[10]T. Omori, M. Fukuda, T. Hirose, Y. Kurihara, R. Kuroda, M. Nomura, A. Ohashi, T. Okugi, K. Sakaue, T. Saito *et al.*, "Efficient propagation of polarization from laser photons to positrons through compton scattering and electron-positron pair creation," Phys. Rev. Lett. **96**, 114801 (2006).

[11]X. Ji, "Deeply virtual compton scattering," Phys. Rev. D **55**, 7114 (1997).

[12]A. P. Potylitsin, "Production of polarized positrons through interaction of longitudinally polarized electrons with thin targets," Nucl. Instrum. Methods Phys. Res., Sect. A **398**, 395–398 (1997).

[13]Y. F. Li, R. Shaisultanov, Y. Y. Chen, F. Wan, K. Z. Hatsagortsyan, C. H. Keitel, and J. X. Li, "Polarized ultrashort brilliant multi-gev γ rays via single-shot laser-electron interaction," Phys. Rev. Lett. **124**, 014801 (2020).

[14]C. Danson, D. Hillier, N. Hopps, and D. Neely, "Petawatt class lasers worldwide," High Power Laser Sci. Eng. **3**, e3 (2015).

[15]V. Yanovsky, V. Chvykov, G. Kalinchenko, P. Rousseau, T. Planchon, T. Matsuoka, A. Maksimchuk, J. Nees, G. Cheriaux, G. Mourou, *et al.*, "Ultra-high intensity-300-TW laser at 0.1 Hz repetition rate," Opt. Express **16**, 2109–2114 (2008).

[16]J. W. Yoon, Y. G. Kim, I. W. Choi, J. H. Sung, H. W. Lee, S. K. Lee, and C. H. Nam, "Realization of laser intensity over 10^{23} W/cm^2," Optica **8**, 630–635 (2021).

[17]See http://www.clf.stfc.ac.uk/Pages/TheVulcan-10-Petawatt-Project.aspx for The Vulcan Facility.

[18]See http://www.elibeams.eu/en/facility/lasers/ for The Extreme Light Infrastructure (ELI).

[19]See http://www.xcels.iapras.ru/ for Exawatt Center for Extreme Light Studies (XCELS).

[20]W. P. Leemans, A. J. Gonsalves, H.-S. Mao, K. Nakamura, C. Benedetti, C. B. Schroeder, C. Tóth, J. Daniels, D. E. Mittelberger, S. S. Bulanov *et al.*, "Multi-GeV electron beams from capillary-discharge-guided subpetawatt laser pulses in the self-trapping regime," Phys. Rev. Lett. **113**, 245002 (2014).

[21]A. J. Gonsalves, K. Nakamura, J. Daniels, C. Benedetti, C. Pieronek, T. C. H. De Raadt, S. Steinke, J. H. Bin, S. S. Bulanov, J. Van Tilborg *et al.*, "Petawatt laser guiding and electron beam acceleration to 8 GeV in a laser-heated capillary discharge waveguide," Phys. Rev. Lett. **122**, 084801 (2019).

[22]V. I. Ritus, "Quantum effects of the interaction of elementary particles with an intense electromagnetic field," J. Sov. Laser Res. **6**, 497–617 (1985).

[23]F. Wan, R. Shaisultanov, Y.-F. Li, K. Z. Hatsagortsyan, C. H. Keitel, and J.-X. Li, "Ultrarelativistic polarized positron jets via collision of electron and ultraintense laser beams," Phys. Lett. B **800**, 135120 (2020).

[24]Y.-Y. Chen, P.-L. He, R. Shaisultanov, K. Z. Hatsagortsyan, and C. H. Keitel, "Polarized positron beams via intense two-color laser pulses," Phys. Rev. Lett. **123**, 174801 (2019).

[25]Y. F. Li, Y. Y. Chen, W. M. Wang, and H. S. Hu, "Production of highly polarized positron beams via helicity transfer from polarized electrons in a strong laser field," Phys. Rev. Lett. **125**, 044802 (2020).

[26]D. Seipt and B. King, "Spin- and polarization-dependent locally-constant-field-approximation rates for nonlinear compton and breit-wheeler processes," Phys. Rev. A **102**, 052805 (2020).

[27]A. Ilderton, B. King, and S. Tang, "Loop spin effects in intense background fields," Phys. Rev. D **102**, 076013 (2020).

[28]V. Dinu and G. Torgrimsson, "Approximating higher-order nonlinear QED processes with first-order building blocks," Phys. Rev. D **102**, 016018 (2020).

[29]G. Torgrimsson, "Loops and polarization in strong-field QED," New J. Phys. **23**, 065001 (2021).

[30]D. Seipt, D. Del Sorbo, C. P. Ridgers, and A. G. Thomas, "Ultrafast polarization of an electron beam in an intense bichromatic laser field," Phys. Rev. A **100**, 061402 (2019).

[31]H.-H. Song, W.-M. Wang, J.-X. Li, Y.-F. Li, and Y.-T. Li, "Spin-polarization effects of an ultrarelativistic electron beam in an ultraintense two-color laser pulse," Phys. Rev. A **100**, 033407 (2019).

[32]Y.-F. Li, R. Shaisultanov, K. Z. Hatsagortsyan, F. Wan, C. H. Keitel, and J.-X. Li, "Ultrarelativistic electron-beam polarization in single-shot interaction with an ultraintense laser pulse," Phys. Rev. Lett. **122**, 154801 (2019).

[33]B. King, N. Elkina, and H. Ruhl, "Photon polarization in electron-seeded pair-creation cascades," Phys. Rev. A **87**, 042117 (2013).

[34]F. Wan, Y. Wang, R.-T. Guo, Y.-Y. Chen, R. Shaisultanov, Z.-F. Xu, K. Z. Hatsagortsyan, C. H. Keitel, and J.-X. Li, "High-energy γ-photon polarization in nonlinear breit-wheeler pair production and γ polarimetry," Phys. Rev. Res. **2**, 032049 (2020).

[35]K. Xue, R.-T. Guo, F. Wan, R. Shaisultanov, Y.-Y. Chen, Z.-F. Xu, X.-G. Ren, K. Z. Hatsagortsyan, C. H. Keitel, and J.-X. Li, "Generation of arbitrarily polarized GeV lepton beams via nonlinear Breit-Wheeler process" (submitted).

[36]I. Gol'dman, "Intensity effects in compton scattering," Sov. Phys.-JETP **19**, 954 (1964).

[37]A. Nikishov and V. Ritus, "Quantum processes in the field of a plane electromagnetic wave and in a constant field. I," Sov. Phys.-JETP **19**, 529–541 (1964).

[38]G. L. Kotkin, V. G. Serbo, and V. I. Telnov, "Electron (positron) beam polarization by Compton scattering on circularly polarized laser photons," Phys. Rev. Spec. Top.-Accel. Beams **6**, 011001 (2003).

[39]D. Y. Ivanov, G. L. Kotkin, and V. G. Serbo, "Complete description of polarization effects in emission of a photon by an electron in the field of a strong laser wave," Eur. Phys. J. C **36**, 127–145 (2004).

[40]D. Y. Ivanov, G. L. Kotkin, and V. G. Serbo, "Complete description of polarization effects in e^+e^- pair productionby a photon in the field of a strong laser wave," Eur. Phys. J. C **40**, 27–40 (2005).

[41]C. P. Ridgers, J. G. Kirk, R. Duclous, T. G. Blackburn, C. S. Brady, K. Bennett, T. D. Arber, and A. R. Bell, "Modelling gamma-ray photon emission and pair production in high-intensity laser–matter interactions," J. Comput. Phys. **260**, 273–285 (2014).

[42]N. Elkina, A. Fedotov, I. Y. Kostyukov, M. Legkov, N. Narozhny, E. Nerush, and H. Ruhl, "QED cascades induced by circularly polarized laser fields," Phys. Rev. Spec. Top.-Accel. Beams **14**, 054401 (2011).

[43]D. G. Green and C. N. Harvey, "SIMLA: Simulating particle dynamics in intense laser and other electromagnetic fields via classical and quantum electrodynamics," Comput. Phys. Commun. **192**, 313–321 (2015).

[44]V. Katkov, V. M. Strakhovenko *et al.*, *Electromagnetic Processes at High Energies in Oriented Single Crystals* (World Scientific, 1998).

[45]V. Dinu, C. Harvey, A. Ilderton, M. Marklund, and G. Torgrimsson, "Quantum radiation reaction: From interference to incoherence," Phys. Rev. Lett. **116**, 044801 (2016).

[46]A. Di Piazza, M. Tamburini, S. Meuren, and C. Keitel, "Implementing nonlinear compton scattering beyond the local-constant-field approximation," Phys. Rev. A **98**, 012134 (2018).

[47]A. Ilderton, B. King, and D. Seipt, "Extended locally constant field approximation for nonlinear compton scattering," Phys. Rev. A **99**, 042121 (2019).

[48]T. Podszus and A. Di Piazza, "High-energy behavior of strong-field QED in an intense plane wave," Phys. Rev. D **99**, 076004 (2019).

[49]A. Ilderton, "Note on the conjectured breakdown of QED perturbation theory in strong fields," Phys. Rev. D **99**, 085002 (2019).
[50]A. Di Piazza, M. Tamburini, S. Meuren, and C. H. Keitel, "Improved local-constant-field approximation for strong-field QED codes," Phys. Rev. A **99**, 022125 (2019).
[51]A. Gonoskov, S. Bastrakov, E. Efimenko, A. Ilderton, M. Marklund, I. Meyerov, A. Muraviev, A. Sergeev, I. Surmin, and E. Wallin, "Extended particle-in-cell schemes for physics in ultrastrong laser fields: Review and developments," Phys. Rev. E **92**, 023305 (2015).
[52]B. King and S. Tang, "Nonlinear compton scattering of polarized photons in plane-wave backgrounds," Phys. Rev. A **102**, 022809 (2020).
[53]T. N. Wistisen and A. Di Piazza, "Numerical approach to the semiclassical method of radiation emission for arbitrary electron spin and photon polarization," Phys. Rev. D **100**, 116001 (2019).
[54]T. N. Wistisen, "Numerical approach to the semiclassical method of pair production for arbitrary spins and photon polarization," Phys. Rev. D **101**, 076017 (2020).
[55]V. N. Baier, V. M. Katkov, and V. M. Strakhovenko, "Quantum radiation theory in inhomogeneous external fields," Nucl. Phys. B **328**, 387 (1989).
[56]T. Blackburn, A. Ilderton, C. Murphy, and M. Marklund, "Scaling laws for positron production in laser–electron-beam collisions," Phys. Rev. A **96**, 022128 (2017).
[57]O. Olugh, Z.-L. Li, B.-S. Xie, and R. Alkofer, "Pair production in differently polarized electric fields with frequency chirps," Phys. Rev. D **99**, 036003 (2019).
[58]L. H. Thomas, "The motion of the spinning electron," Nature **117**, 514 (1926).
[59]L. H. Thomas, "I. The kinematics of an electron with an axis," London, Edinburgh Dublin Philos. Mag. J. Sci. **3**, 1–22 (1927).
[60]V. Bargmann, L. Michel, and V. L. Telegdi, "Precession of the polarization of particles moving in a homogeneous electromagnetic field," Phys. Rev. Lett. **2**, 435 (1959).
[61]K. Xue, Z.-K. Dou, F. Wan, T.-P. Yu, W.-M. Wang, J.-R. Ren, Q. Zhao, Y.-T. Zhao, Z.-F. Xu, and J.-X. Li, "Generation of highly-polarized high-energy brilliant γ-rays via laser-plasma interaction," Matter Radiat. Extremes **5**, 054402 (2020).
[62]R.-T. Guo, Y. Wang, R. Shaisultanov, F. Wan, Z.-F. Xu, Y.-Y. Chen, K. Z. Hatsagortsyan, and J.-X. Li, "Stochasticity in radiative polarization of ultrarelativistic electrons in an ultrastrong laser pulse," Phys. Rev. Res. **2**, 033483 (2020).